PCCP

PAPER

CrossMark
click for updates

Mechanistic aspects of the gas-phase coupling of thioanisole and chlorobenzene to dibenzothiophene catalyzed by atomic Ho+†‡

Shaodong Zhou, Maria Schlangen and Helmut Schwarz*

Mechanistic aspects of the novel gas-phase generation of dibenzothiophene *via* coupling of thioanisole and chlorobenzene, employing atomic Ho+ as a catalyst, have been investigated using Fourier-transform ion cyclotron resonance mass spectrometry in conjunction with density functional theory (DFT) calculations.

Introduction

Sulfur heterocycles are important building blocks of various chemical products, including organic thin-film transistors,[1,2] metal extracting reagents,[3,4] or bioactive and medicinally relevant compounds.[5–8] Consequently, methodological aspects related to the formation of organosulfur heterocyclic rings have attracted much attention. For the synthesis of sulfur-containing heterocycles usually metal sulfides, thioesters, or thioethers are employed as starting materials, and first- or second-row transition-metal complexes serve as catalysts. To achieve C–C[9–12] or C–S[13–20] coupling involved in the ring closure process, activation of C–H,[9–20] C–X (X = Br or I)[15,18,20] or C–S[14,17] bonds is a prerequisite. While gas-phase investigations proved helpful to obtain mechanistic aspects for numerous processes, except for a few reports on the formation of sulfur heterocycles in the gas phase,[21] a more detailed understanding of the elementary steps is lacking.

In a previous study on the reactions of atomic Ln+ with chlorobenzene,[22] strong indications have been found that Ho+ generates efficiently the insertion product Ho(C$_6$H$_5$)(Cl)+ which then promotes HCl elimination in a secondary reaction with chlorobenzene; further, intriguing coupling processes have been observed in preliminary studies on consecutive reactions of Ln+ with chlorobenzene and thioanisole in which Ho+ exhibited the highest efficiency. Thus, we explored these reactions in more detail, and here we describe a gas-phase approach of sequential C–C and C–S coupling to generate dibenzothiophene by using thioanisole and chlorobenzene as substrates and exploiting atomic Ho+ as a catalyst. Gas-phase studies employing atomic
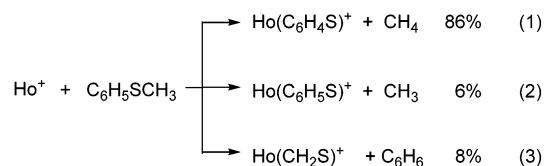
catalysts[23] recently regained interest[24] in the context of "single-atom catalysis".[25]

Results and discussion

Coupling of thioanisole and chlorobenzene is achieved *via* two steps: first, Ho+ reacts with thioanisole to produce an ionic precursor, which subsequently undergoes reaction with chlorobenzene to re-generate Ho+ under the elimination of the neutral heterocyclic product.

1 Reactions of Ho+ with thioanisole

1.1 Ion–molecule reactions of Ho+ with thioanisole. Three primary channels were observed in the thermal reaction of Ho+ with thioanisole introduced *via* a leak valve at a stationary pressure of $p = 1.0 \times 10^{-8}$ bar, *i.e.* reactions (1)–(3); the overall efficiency amounts to 30%, relative to the collision rate.[26]

$$\text{Ho}^+ + \text{C}_6\text{H}_5\text{SCH}_3 \longrightarrow \begin{cases} \text{Ho(C}_6\text{H}_4\text{S)}^+ + \text{CH}_4 & 86\% \quad (1) \\ \text{Ho(C}_6\text{H}_5\text{S)}^+ + \text{CH}_3 & 6\% \quad (2) \\ \text{Ho(CH}_2\text{S)}^+ + \text{C}_6\text{H}_6 & 8\% \quad (3) \end{cases}$$

C–S bond activation is involved in all three channels; in addition, C–H bond activation takes place in reactions (1) and (3), respectively. Structural information on the cationic product ions as well as mechanistic aspects of these processes were obtained from DFT calculations. The potential-energy surfaces (PESs) together with structural data of the associated intermediates and transition structures are shown in Fig. 1 for the generations of Ho(C$_6$H$_4$S)+ and Ho(C$_6$H$_5$S)+, and in Fig. 2 two alternative pathways for the formation of Ho(CH$_2$S)+ are presented.

1.2 Pathways to form Ho(C$_6$H$_4$S)+ and Ho(C$_6$H$_5$S)+. Several coordination modes, *e.g.* η^2 or η^6 coordination to the ring,

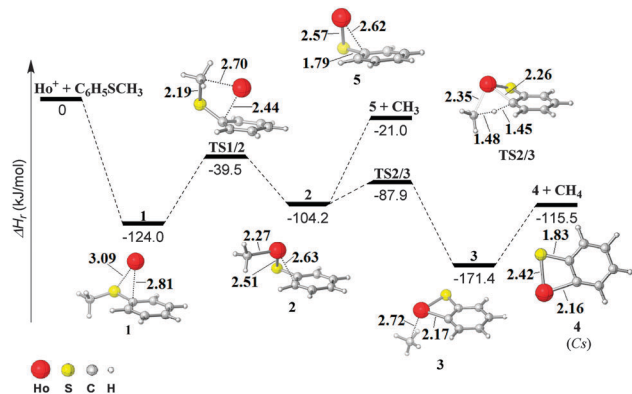*Institut für Chemie, Technische Universität Berlin, Straße des 17. Juni 135, 10623 Berlin, Germany. E-mail: helmut.schwarz@tu-berlin.de*

Fig. 1 PESs and structural information of the associated coordinates for the generations of $Ho(C_6H_4S)^+$ and $Ho(C_6H_5S)^+$. Selected bond lengths are given in Å; for the sake of clarity, charges are omitted.
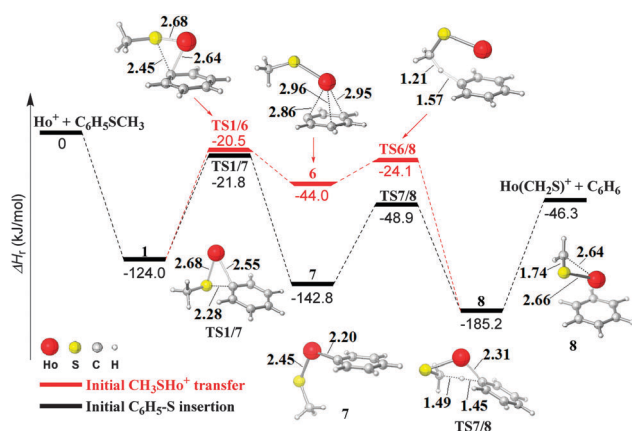

Fig. 2 PESs and structural information of the associated coordinates for the generation of $Ho(CH_2S)^+$. Selected bond lengths are given in Å; for the sake of clarity, charges are omitted.
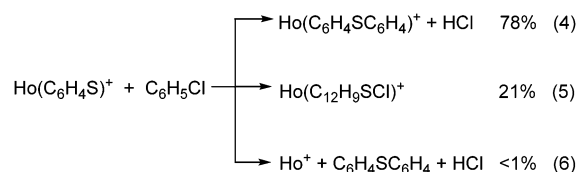
attachment of the cation to the sulfur atom *etc.*, have been taken into account for the generation of an encounter complex of Ho^+ with thioanisole; however, irrespective of all starting structures considered, as a result of the optimization, only **1** has been identified as encounter complex. In **1**, Ho^+ is η^2 coordinated to the sulfur and the *ipso*-carbon atom of the phenyl ring. This intermediate serves as the starting point for all three reaction channels (1)–(3). Subsequent to the adduct formation, the generations of both $Ho(C_6H_4S)^+$ and $Ho(C_6H_5S)^+$, reactions (1) and (2), proceed by the oxidative insertion of Ho^+ into the $S–CH_3$ bond thus forming intermediate **2**. Since ground state Ho^+ possesses a $4f^{11}5d^06s^1$ electronic configuration, one 4f electron of Ho^+ has to be promoted to a non-f valence orbital to allow the formation of **2** in which holmium is engaged in forming two σ bonds. NBO analysis of the IRC coordinates of **TS1/2** indicates that the electron promotion of Ho^+ from a 4f orbital to a non-f valence orbital occurs after cleavage of the $S–CH_3$ bond. Thus, both the promotion energy (PE) of Ho^+ to attain a $4f^{10}5d^16s^1$ configuration (158 kJ mol^{-1} (ref. 27)) as well as the $S–CH_3$ bond dissociation energy ($BDE(S–CH_3)$, 278 kJ mol^{-1} (ref. 28)) accompanied by distortion of the anisole molecule

contribute to the energy barrier associated with **TS1/2**. While the homolytic cleavage of the $Ho–CH_3$ bond of intermediate **2** results in the formation of holmium benzenethiolate $Ho(C_6H_5S)^+$ (**5**), generation of $Ho(C_6H_4S)^+$ (**4**) proceeds *via* a metal mediated σ-bond metathesis process **2** → **3**, in which a hydrogen-atom transfer takes place from the *ortho*-position of the phenyl ring to the methyl group *via* **TS2/3**. Subsequently, the elimination of methane gives rise to the product ion **4**. In line with the experimental results, both reactions are exothermic and thus energetically accessible under thermal conditions; moreover, the preferred elimination of CH_4, observed in the experiments, agrees with the more energy demanding cleavage of the $Ho–CH_3$ bond of **2**, accompanied with the generation of $Ho(C_6H_5S)^+$, as compared to the liberation of CH_4 along the sequence **2** → **3** → **4**. Considering the relative energies of **TS2/3** and **TS1/2** (-87.9 kJ mol^{-1} *versus* -39.5 kJ mol^{-1}), insertion of Ho^+ into the $S–CH_3$ bond constitutes the rate-limiting step for the generation of the major product $Ho(C_6H_4S)^+$.

1.3 Generation of $Ho(CH_2S)^+$. Two pathways have been located to produce $Ho(CH_2S)^+$. The first one commences with insertion of Ho^+ into the $S–C_6H_5$ bond, while in the second one the CH_3S group remains bound in the migration of Ho^+ to the top of the phenyl ring. As mentioned above, for the insertion process one electron of Ho^+ has to be promoted from a 4f orbital to a non-f valence orbital; according to NBO analysis, the promotion takes place in proceeding from **TS1/7** to intermediate **7** after cleavage of the $S–C_6H_5$ bond; then, again, one electron re-occupies the 4f orbital of Ho^+ in the step **TS7/8** → **8**. In contrast, a 4f → non-f promotion is not necessary for the pathway initiated by migration of the whole CH_3SHo^+ unit; here, throughout the reaction sequence **1** → **6** → **8** the holmium atom remains covalently bound only to the sulfur atom. Considering the comparable energies of **TS1/6**, **TS1/7**, and **TS6/8**, generation of $Ho(CH_2S)^+$ is influenced by several factors, including the $BDE(C_6H_5–S)$ (357 kJ mol^{-1} (ref. 28)), and $BDE(Ho^+SCH_2–H)$, as well as the PE of Ho^+ to attain a $4f^{10}5d^16s^1$ configuration. Finally, compared to the formation of $Ho(C_6H_4S)^+$, the generation of $Ho(CH_2S)^+$ is energetically less favorable, in agreement with its lower branching ratio; also, the energetics for the generations of $Ho(C_6H_5S)^+$ and $Ho(CH_2S)^+$ are in line with their similar branching ratios.

2 Reactions of $Ho(C_6H_4S)^+$ with chlorobenzene

For probing the thermal reactions of $Ho(C_6H_4S)^+$ with chlorobenzene, the thermalized, mass-selected precursor $Ho(C_6H_4S)^+$ is exposed to chlorobenzene which is introduced *via* a leak valve and present in the ICR cell at a stationary pressure of $p = 1.0 \times 10^{-8}$ bar. The overall reaction efficiency amounts to 7%, and three primary product channels were observed, *i.e.* reaction (4)–(6). Performing the same experiments without thermalization of

$$Ho(C_6H_4S)^+ + C_6H_5Cl \longrightarrow
\begin{cases}
Ho(C_6H_4SC_6H_4)^+ + HCl & 78\% \quad (4) \\
Ho(C_{12}H_9SCl)^+ & 21\% \quad (5) \\
Ho^+ + C_6H_4SC_6H_4 + HCl & <1\% \quad (6)
\end{cases}$$

the precursor $Ho(C_6H_4S)^+$, the branching ratio of reaction (6) increases up to 27%, while the branching ratios of reaction (4) and (5) decrease to 63% and 10%, respectively.

The assignment of the $[C_{12},H_8,S]$ unit as a dibenzothiophene ligand $(C_6H_4SC_6H_4)$ in the product ion of reaction (4) as well as for the neutral molecule of reaction (6) is based on the following considerations. First, if $[C_{12},H_8,S]$ corresponds to an intact $[C_{12},H_8,S]$ ligand we assume a dibenzothiophene structure since the generation of isomeric naphthothiophene is much more complicated starting from the two substrates employed in the experiments. The next and even more important aspect concerns the question if $[C_{12},H_8,S]$ represents a single ligand, or if it is composed of two individual units, *e.g.* C_6H_4S and C_6H_4. To this end, the major product ion $Ho(C_{12}H_8S)^+$ has been mass selected and subjected to collision-induced dissociation (CID). At a collision energy $E_{coll} = 3.6$ eV (given in the center-of-mass frame), Ho^+ and HoS^+ are produced upon collision with argon in a ratio of about $9:1$; applying lower collision energies, Ho^+ corresponds to the only fragment ion generated. From the above results, the following conclusions can be drawn: (i) $Ho(C_{12}H_8S)^+$ corresponds to a complex with a single ligand which we assign to dibenzothiophene; the latter is generated in the reaction of thermalized $Ho(C_6H_4S)^+$ with chlorobenzene under the elimination of HCl, and (ii) "bare" Ho^+ is formed as product ion *via* the consecutive eliminations of HCl and dibenzothiophene. Further, the alternative formation of $[Ho(C_6H_4S)(C_6H_4)]^+$, possessing two individual ligands, *e.g.* C_6H_4S and benzyne, would result in the formations of both fragment ions $Ho(C_6H_4S)^+$ and $Ho(C_6H_4)^+$ upon CID. Moreover, the generation of the $Ho(C_6H_4S)(C_6H_4)^+$ + HCl is, according to the calculation, endothermic by 190.1 kJ mol^{-1} (for more structural details of $Ho(C_6H_4S)(C_6H_4)^+$, see ESI‡). Finally, the possible charge transfer product, $C_6H_4SC_6H_4^+$, was not observed, in line with the much higher ionization energy of dibenzothiophene (8.44 eV[29]) as compared to that of holmium (6.0 eV[30]).

Two chemically plausible pathways, (a) and (b), are proposed for the generation of $Ho(C_6H_4SC_6H_4)^+$ possessing a $C_6H_4SC_6H_4$ ligand as illustrated in Scheme 1; both routes are initiated by σ bond metathesis under cleavage of the Ho–S and Ho–C bonds of the complex $Ho(C_6H_4S)^+$, respectively. The PESs and the structural information of the associated intermediates and transition structures for the two pathways are shown in Fig. 3, and the encounter complex **9** serves as a common starting point. The TS for the Ho–S bond cleavage (**TS9/10**) is much higher in energy relative to the entrance channel as well as to the alternative Ho–C
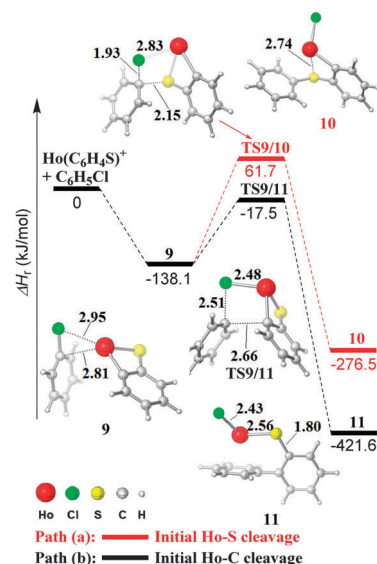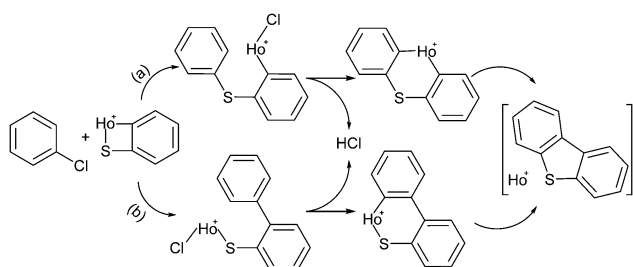

Fig. 3 PESs and structural information of the associated coordinates for the initial Ho–C and Ho–S cleavages of $Ho(C_6H_4S)^+$ upon its reaction with chlorobenzene. Selected bond lengths are given in Å; charges are omitted for the sake of clarity.

bond cleavage proceeding *via* **TS9/11** (61.7 kJ mol^{-1} *versus* −17.5 kJ mol^{-1}), *i.e.* dehydrochlorination is accessible under thermal conditions only *via* path (b) (**9** → **TS9/11** → **11**); therefore, it is only this route which has been considered further in the calculations of the subsequent reaction steps. The reason for the much higher barrier of the Ho–S bond cleavage (**TS9/10**) as compared to the Ho–C bond (**TS9/11**) is probably related to the stronger Ho–S bond compared to the Ho–C bond reflecting electronegativity differences between sulfur and carbon; unfortunately, the respective bond-dissociation energies are not reported in the literature.

Subsequent to the formation of intermediate **11**, dehydrochlorination proceeds either directly *via* a hydrogen atom transfer from an *ortho*-position of the phenyl ring to the chloride ligand (**11** → **12**), or may be preceded by hydrogen scrambling within the original chlorobenzene entity (**11** → **13** → **14** → **15** → **16**). The PESs for these processes and structural information of the associated intermediates and transition structures for the generation of $Ho(C_6H_4SC_6H_4)^+$ as well as the intermediates for hydrogen scrambling along **13** ⇌ ⇌ **16** are shown in Fig. 4; structural details of the transition structures involved in the hydrogen scrambling are given in ESI.‡ According to the calculations, hydrogen scrambling is less energy demanding than the loss of HCl. The H/D scrambling has been verified by labeling experiments: in the reactions of $Ho(C_6H_4S)^+$ with 3,5-d_2-1-chlorobenzene and 4-d-1-chlorobenzene, eliminations of both HCl and DCl are observed for either substrate; the ratios of HCl/DCl elimination from 3,5-d_2-1-chlorobenzene and from 4-d-1-chlorobenzene amount to $84:16$ and $87:13$, respectively. To quantitatively analyse these results in a kinetic modeling,[31–35] hydrogen migration along the phenyl ring is treated as a complete H/D scrambling processes; further, the ratio for a *direct* HCl/DCl elimination *versus* H/D scrambling prior to HCl/DCl elimination as well as a kinetic isotope effect (KIE) have been fitted to the experimental data for

Scheme 1 Plausible pathways for the generation of $Ho(C_6H_4SC_6H_4)^+$.

9566 | *Phys. Chem. Chem. Phys.*, 2015, **17**, 9564–9568

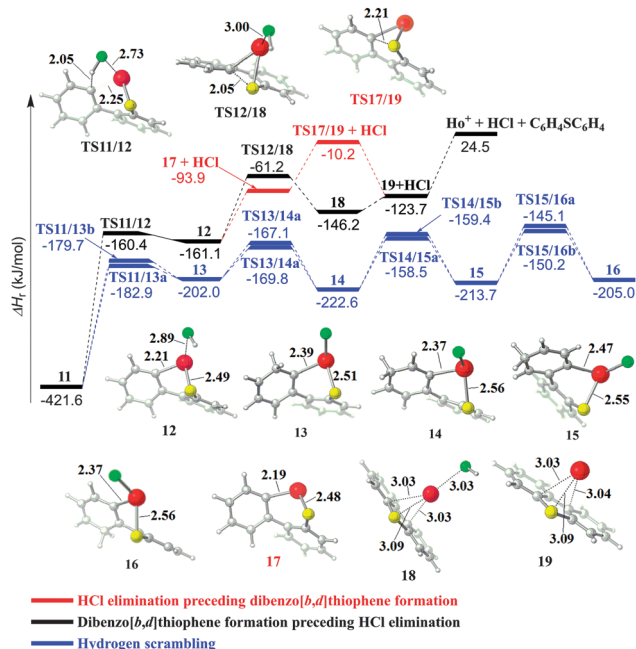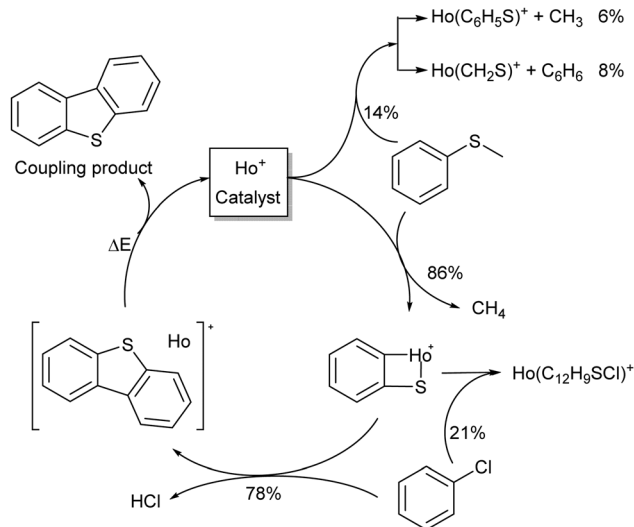This journal is © the Owner Societies 2015

Fig. 4 PESs of the reactions starting from intermediate **11** as well as the structural information of some key coordinates; the notations a and b for the transition structures stand for the hydrogen migrations on both sites of the ring, respectively. Selected bond lengths are given in Å; charges are omitted for the sake of clarity. For further structural information, see Fig. S2 of ESI.‡

both isotopologues. It turned out that the experimental data can be best modeled with assuming KIE = 1 and a branching ratio of 45% for H/D scrambling processes *versus* direct HCl/DCl elimination. A KIE = 1 is in agreement with the theoretical results, in that C–H(D) bond activation does not correspond to the rate-limiting step in the liberation of H(D)Cl and the generation of $Ho(C_6H_4SC_6H_4)^+$.

After having formed **12**, the next step corresponds to the construction of the thiophene ring; there are two variants in regard to the loss of HCl which can occur before or after the ring closure. The direct formation of the thiophene ring proceeds *via* **TS12/18** to form **18**, and subsequent elimination of HCl generates **19**; alternatively, direct liberation of HCl from **12** gives rise to **17** which subsequently rearranges *via* **TS17/19** to the complex **19** (see Fig. 4); both processes are accessible at thermal conditions. Thus, according to the calculation, the observed ionic product $Ho(C_6H_4SC_6H_4)^+$ may correspond to a mixture of **17** and **19**. Regarding the formation of $Ho^+ + HCl + C_6H_4SC_6H_4$, reaction (6), this has been calculated to be higher in energy by 25 kJ mol^{-1} as compared to the entrance channel, *i.e.* $Ho(C_6H_4S)^+ + C_6H_5Cl$, and should thus not be observed under thermal conditions. Thus, assuming that the ions in the experiments are thermalized to room temperature possessing a kinetic energy of $3RT = 7.4$ kJ mol^{-1} at 298 K, theory overestimates the relative energy of the exit channel.

Considering the overall process, *i.e.* $Ho^+ + C_6H_5SCH_3 + C_6H_5Cl \rightarrow Ho^+ + HCl + C_6H_4SC_6H_4$, the atomic holmium cation Ho^+ serves as a catalyst, as illustrated in Scheme 2. However, the turnover number is limited by side reactions with both substrates

(processes (2), (3), and (5)), and the turn-over frequency is diminished due to the inefficient release of the neutral coupling product from **19** under the regeneration of Ho^+ ions to initiate the next catalytic cycle. As so often in heterogeneous catalysis, product release and regeneration of the active catalyst (*i.e.* Ho^+) requires external energy.[36–41] In addition, the presence of both substrates thioanisole and chlorobenzene at the same time in a "one-pot synthesis" allows for additional side reactions as Ho^+ can react with both precursors. Moreover, $Ho(C_6H_4S)^+$ can also react further with thioanisole to give higher order products. Thus, timing of the interaction of the catalyst with the two substrates needs to be well designed to improve the efficiency of the coupling process.

Scheme 2 Catalytic cycle for the coupling of thioanisole and chlorobenzene mediated by atomic Ho^+ as well as side reactions.

Conclusion

In this work, we present a novel gas-phase coupling of thioanisole and chlorobenzene to dibenzothiophene catalyzed by "bare" holmium cation Ho^+ and we address mechanistic aspects by DFT calculations and labeling experiments. The coupling is achieved *via* a two-step reaction: the first one corresponds to the reaction of Ho^+ with thioanisole to generate $Ho(C_6H_4S)^+$; subsequently, $Ho(C_6H_4S)^+$ reacts with chlorobenzene to produce the final products. A combination of experimental and computational investigations, provides insight into the most likely reaction mechanisms. For the overall transformation, atomic Ho^+ serves as a catalyst which, however, is also engaged in side reactions with both substrates. Similar to heterogeneous catalysis, external energy is required to release the coupling product from the catalyst.

Acknowledgements

This journal is © the Owner Societies 2015

Phys. Chem. Chem. Phys., 2015, **17**, 9564–9568 | 9567

Notes and references

1 P. Y. Huang, L. H. Chen, Y. Y. Chen, W. J. Chang, J. J. Wang, K. H. Lii, J. Y. Yan, J. C. Ho, C. C. Lee, C. Kim and M. C. Chen, *Chem. – Eur. J.*, 2013, **19**, 3721–3728.

2 E. L. Ratcliff, R. C. Bakus, G. C. Welch, T. S. van der Poll, A. Garcia, S. R. Cowan, B. A. MacLeod, D. S. Ginley, G. C. Bazan and D. C. Olson, *J. Mater. Chem. C*, 2013, **1**, 6223–6234.

3 C. Freund, W. Porzio, U. Giovanella, F. Vignali, M. Pasini, S. Destri, A. Mech, S. Di Pietro, L. Di Bari and P. Mineo, *Inorg. Chem.*, 2011, **50**, 5417–5429.

4 C. Greco, G. Moro, L. Bertini, M. Biczysko, V. Barone and U. Cosentino, *J. Chem. Theory Comput.*, 2014, **10**, 767–777.

5 C. D. Jones, M. G. Jevnikar, A. J. Pike, M. K. Peters, L. J. Black, A. R. Thompson, J. F. Falcone and J. A. Clemens, *J. Med. Chem.*, 1984, **27**, 1057–1066.

6 J. K. Chakrabarti, T. M. Hotten and D. E. Tupper, US5229382A, 1990.

7 S. Martin-Santamaria, J. J. Rodriguez, S. de Pascual-Teresa, S. Gordon, M. Bengtsson, I. Garrido-Laguna, B. Rubio-Viqueira, P. P. Lopez-Casas, M. Hidalgo, B. de Pascual-Teresa and A. Ramos, *Org. Biomol. Chem.*, 2008, **6**, 3486–3496.

8 E. Bey, S. Marchais-Oberwinkler, M. Negri, P. Kruchten, A. Oster, T. Klein, A. Spadaro, R. Werth, M. Frotscher, B. Birk and R. W. Hartmann, *J. Med. Chem.*, 2009, **52**, 6724–6743.

9 A. R. Katritzky, R. A. Barcock, E. S. Ignatchenko, S. M. Allin, M. Siskin and C. W. Hudson, *Energy Fuels*, 1997, **11**, 150–159.

10 C. L. Sun, Y. F. Gu, W. P. Huang and Z. J. Shi, *Chem. Commun.*, 2011, **47**, 9813–9815.

11 R. Samanta and A. P. Antonchick, *Angew. Chem., Int. Ed.*, 2011, **50**, 5217–5220.

12 R. Che, Z. Wu, Z. Li, H. Xiang and X. Zhou, *Chem. – Eur. J.*, 2013, **20**, 7258–7261.

13 Y. L. Mao and V. Boekelheide, *Proc. Natl. Acad. Sci. U. S. A.*, 1980, **77**, 1732–1735.

14 M. Black, J. I. G. Cadogan and H. Mcnab, *J. Chem. Soc., Chem. Commun.*, 1990, 395–396.

15 L. Benati, R. Leardini, M. Minozzi, D. Nanni, P. Spagnolo, S. Strazzari and G. Zanardi, *Org. Lett.*, 2002, **4**, 3079–3081.

16 G. K. S. Prakash, C. Weber, S. Chacko and G. A. Olah, *Org. Lett.*, 2007, **9**, 1863–1866.

17 M. Black, J. I. G. Cadogan and H. Mcnab, *Org. Biomol. Chem.*, 2010, **8**, 2961–2967.

18 W. You, X. Y. Yan, Q. A. Liao and C. J. Xi, *Org. Lett.*, 2010, **12**, 3930–3933.

19 T. H. Jepsen, M. Larsen, M. Jorgensen, K. A. Solanko, A. D. Bond, A. Kadziola and M. B. Nielsen, *Eur. J. Org. Chem.*, 2011, 53–57.

20 Z. J. Qiao, H. Liu, X. Xiao, Y. N. Fu, J. P. Wei, Y. X. Li and X. F. Jiang, *Org. Lett.*, 2013, **15**, 2594–2597.

21 M. M. Basher, Y. E. Corilo, R. Sparrapan, M. Benassi, R. Augusti, M. N. Eberlin and J. M. Riveros, *J. Mass Spectrom.*, 2012, **47**, 1526–1535.

22 S. Zhou, M. Schlangen and H. Schwarz, *Chem. – Eur. J.*, 2015, **21**, 2123–2131.

23 D. K. Bohme and H. Schwarz, *Angew. Chem., Int. Ed.*, 2005, **44**, 2336–2354.

24 H. Schwarz, *Isr. J. Chem.*, 2014, **54**, 1413–1431.

25 X. F. Yang, A. Q. Wang, B. T. Qiao, J. Li, J. Y. Liu and T. Zhang, *Acc. Chem. Res.*, 2013, **46**, 1740–1748.

26 M. T. Bowers and J. B. Laudenslager, *J. Chem. Phys.*, 1972, **56**, 4711–4712.

27 V. Blagojevic, E. Flaim, M. J. Y. Jarvis, G. K. Koyanagi and D. K. Bohme, *Int. J. Mass Spectrom.*, 2006, **249**, 385–391.

28 Y.-R. Luo, *Comprehensive Handbook of Chemical Bond Energies*, CRC Press, Boca Raton, 2007.

29 J. K. Terlouw, W. Heerma, P. C. Frintrop, G. Dijkstra and H. A. Meinema, *J. Organomet. Chem.*, 1974, **64**, 205–221.

30 R. J. Ackermann, E. G. Rauh and R. J. Thorn, *J. Chem. Phys.*, 1976, **65**, 1027–1031.

31 D. Schroder and H. Schwarz, *Angew. Chem., Int. Ed.*, 1990, **29**, 1431–1433.

32 D. Schroder, R. Brown, P. Schwerdtfeger and H. Schwarz, *Int. J. Mass Spectrom.*, 2000, **203**, 155–163.

33 J. R. Brown, P. Schwerdtfeger, D. Schroder and H. Schwarz, *J. Am. Soc. Mass Spectrom.*, 2002, **13**, 485–492.

34 J. Loos, D. Schroder and H. Schwarz, *J. Org. Chem.*, 2005, **70**, 1073–1076.

35 B. Butschke, D. Schroder and H. Schwarz, *Organometallics*, 2009, **28**, 4340–4349.

36 C. Bianchini, K. G. Caulton, C. Chardon, O. Eisenstein, K. Folting, T. J. Johnson, A. Meli, M. Peruzzini, D. J. Rauscher, W. E. Streib and F. Vizza, *J. Am. Chem. Soc.*, 1991, **113**, 5127–5129.

37 R. Wesendrup and H. Schwarz, *Organometallics*, 1997, **16**, 461–466.

38 B. Chiavarino, M. E. Crestoni and S. Fornarini, *Chem. – Eur. J.*, 2002, **8**, 2740–2746.

39 T. Waters, R. A. J. O'Hair and A. G. Wedd, *J. Am. Chem. Soc.*, 2003, **125**, 3384–3396.

40 S. M. Lang, T. M. Bernhardt, R. N. Barnett and U. Landman, *Angew. Chem., Int. Ed.*, 2010, **49**, 980–983.

41 A. A. Lysova and I. V. Koptyug, *Chem. Soc. Rev.*, 2010, **39**, 4585–4601.

9568 | *Phys. Chem. Chem. Phys.*, 2015, **17**, 9564–9568

This journal is © the Owner Societies 2015